Late Holocene cyclic glaciomarine sedimentation in a subpolar fjord of the South Shetland Islands, Antarctica, and its paleoceanographic significance: Sedimentological, geochemical, and paleontological evidence

Ho Il Yoon[1,†], Kyu-Cheul Yoo[1], Young-Suk Bak[2], Hyoun Soo Lim[1], Yeadong Kim[1], and Jae Il Lee[1]
[1]*Korea Polar Research Institute of Korea Ocean Research and Development Institute, Songdo Techno Park, Incheon, 406-840, Korea*
[2]*Department of Geology, Kyungpook National University, Taegu 702-701, Korea*

ABSTRACT

The glaciomarine sedimentary record of the fjord head (Collins Harbor) in Maxwell Bay, South Shetland Islands (West Antarctica), a large marine calving embayment, contains repeating couplets of organic-rich massive diamicton and organic-poor stratified diamicton. The massive diamicton is characterized by high total organic carbon (TOC) content and carbon to nitrogen (C/N) ratios and was deposited in a cold climate regime by iceberg-rafted sedimentation from coastal fast ice in which algal plants, as well as gravels, were entrained. The stratified diamicton is characterized by low TOC content and C/N ratios and was formed in a warmer climate regime when the flux of icebergs was suppressed, but turbid meltwater discharge continued to produce lamination. When the meltwater discharge decreased in cold climatic conditions, and resultant phytoplankton productivity was reduced due to the increased sea-ice coverage, ice rafting from shorefast sea ice might have played a major role in entraining benthic algae, as well as loads of sand and gravel, along the coastal area, resulting in an increased C/N ratio and gravel content in the massive diamicton. Accelerator mass spectrometry (AMS) radiocarbon analyses conducted on well-preserved calcite shells were used to construct a chronology for the past 3000 years. Fluctuations in TOC are recorded (approximately four cycles over this time period), with the average duration of a cooling cycle being ~500 years. These cycles may be correlative with the high-frequency (550 yr) variability in reduced Circumpolar Deep Water (CDW) on the West Antarctic Peninsula shelf, because a decrease in CDW may be related to reduced deep water production in the North Atlantic during colder periods, as demonstrated for glacial intervals throughout the Pleistocene.

INTRODUCTION

A substantial body of literature has been compiled on northern high-latitude fjords, particularly those of the Canadian Arctic, Greenland, and Scandinavia. Bays and fjords are important components of the glacial-marine environment of the South Shetland Islands, Antarctica, but only recently have they been studied in detail. The fjords and bays of the South Shetland Islands are located in a relatively warm and humid climatic regime (Reynolds, 1981), producing a temperate glacial setting in which bay waters are turbid with terrigenous debris during the austral summer (Yoon et al., 1998). The stability of valley glaciers and/or tidewater glaciers in this region is thus affected by changes in ablation and in the amount of glacier meltwater, which is closely associated with climate in the region. Recent studies have revealed that substantial retreat in the frontal position of the glacier in Marian Cove (the largest marine calving embayment of Maxwell Bay in the South Shetland Islands) during the past 50 years has been largely due to atmospheric warming (Park et al., 1998).

Alternatively, or in concert, the bay water temperature and the current regime may play a critical role in the distribution of sea ice and glacier front stability. The bay water in Maxwell Bay is influenced by strong warm (~1.3 °C) water intrusion in the late summer derived from Circumpolar Deep Water (CDW) (Chang et al., 1990). Because this relatively warm CDW may provide a heat source to surface waters (Hofmann et al., 1996), a change in the intensity of CDW, driven by either local or global events, can potentially determine sea-ice extent and corresponding glacier front stability in this region. Hence, the past fluctuations in biogenic sedimentary components, sand, and other terrigenous components in the glaciomarine deposits accumulating seaward of the glacier front during the past several thousand years may reflect the changing influence of CDW in the bay waters of the northern Antarctic Peninsula. During the austral summer of 2002–2003, the R/V *Yuzhmogeogiya* collected sediment cores very close to a glacier front at the fjord head of Maxwell Bay. The purpose of the study was to determine the late Holocene history of glacier front fluctuations recorded in glaciomarine sediments from a fjord head (Collins Harbor) in Maxwell Bay, South Shetland Islands, which may demonstrate the significance of short-term climatic cycles that are most likely global in nature.

ENVIRONMENTAL CHARACTERISTICS

Climate, Sea-Ice Distribution, and Glacial Setting

The South Shetland Islands, including Maxwell Bay, experience a slightly more moderate climate (cold temperate to subpolar) than the nearby Antarctic Peninsula region because of their lower latitude. The mean summer temperature varies from 1.1 °C (December) to 2.2 °C (January) with a mean summer relative humidity of 89%, resulting in high surface melting and runoff (KOPRI, 2009). Late summer snow lines around the study area are at ~150 m. Basal ice temperatures are unknown but are likely to be at the pressure melting point near glacier termini, since basal temperatures in glaciers farther south are known to be at the pressure melting point (Smith, 1972). Evidence of regional atmospheric warming was found by comparison of aerial photographs of Marian Cove, a tributary embayment of Maxwell Bay (Park et al., 1998), indicating that the rate of glacier retreat between 1989 and 1994 was approximately the same as

†E-mail: hiyoon@kopri.re.kr

GSA Bulletin; July/August 2010; v. 122; no. 7/8; p. 1298–1307; doi: 10.1130/B30178.1; 7 figures; 1 table.

that during the former 30 years (1956–1986). The high summer temperature (up to 2.0 °C) around Maxwell Bay is responsible for the relatively high rates of meltwater production and sediment supply (Yoon et al., 1998). Annual total rainfall is ~17 cm, and rainfall during the austral summer (from December to February) accounts for 73% of the total annual rainfall. Annual total snowfall is ~1059 cm in water equivalent, and monthly total snowfall reached a maximum value of 418 cm in October 2007 (KOPRI, 2009). Pack ice in Maxwell Bay begins to form in August, and from late October it rapidly breaks up and the bay soon becomes completely ice free, giving rise to increased productivity. Furthermore, modern Maxwell Bay frequently remains ice free throughout the whole year due to the recent regional atmospheric warming (Vaughan et al., 2003). This is important because the ice-free condition permits a continuous supply of light to phytoplankton throughout the entire year. In addition, without coastal sea ice, little ice rafting and scouring of coastal algal plants and/or beach gravel and sand take place. Marine benthic algal flora from Maxwell Bay is dominated by brown algae, Phaeophyta *Himantothallus grandifolius*, and red algae, Rhodophyta *Curdiea racovitzae* (Kim et al., 2001).

Glaciers in Maxwell Bay belong to relatively thin ice fields that in many cases terminate on land. Most of the coastlines are therefore gravel and sand beaches in summer (Fig. 1). In the austral winter, coastal sea ice commonly contains algal material and gravel on its onshore margin (Yoon et al., 1998). The surfaces of glaciers and extensive ice walls, which are mostly confined to the heads of the fjords, are heavily crevassed and covered by silt-sized volcanic material of eolian origin (Fig. 2). Meltwater streams form small outwash fans along the fjord walls of Maxwell Bay (Fig. 1).

Oceanography

Maxwell Bay opens directly to the Bransfield Strait, which receives a variety of water types from the Bellingshausen and Weddell seas. The presence of a deep sill (450 m) allows for active subsurface water exchange, and Collins Harbor can easily be affected by open ocean conditions. During the winter, the entire water column of Maxwell Bay is <0 °C; this is referred to as Winter Water (Chang et al., 1990). However, during the summer and fall, increased solar insolation and intrusion of warm subsurface water changes the water column structure of Maxwell Bay, although the bottom water retains some of the temperature and salinity characteristics of winter conditions. Near the head of the bay, a cold, fresh, and turbid surface layer is evident, a result of the input of glacially derived meltwater. Surface heating warms the surface water and isolates a core of Antarctic Surface Water as a remnant of Winter Water. Below this, a temperature maximum layer appears, extending to ~50 m in the ice proximal area of Maxwell Bay. Strong warm water intrusion in the late summer (1.3 °C, 33.80 psu) is derived from the Antarctic waters north of the Antarctic Circumpolar Current (ACC) (Read et al., 1995; Yoo et al., 2002). The observed inflow is associated with the shallow intrusions of Circumpolar Deep Water (CDW) into Maxwell Bay from the Drake Passage (Chang et al., 1990). During the late

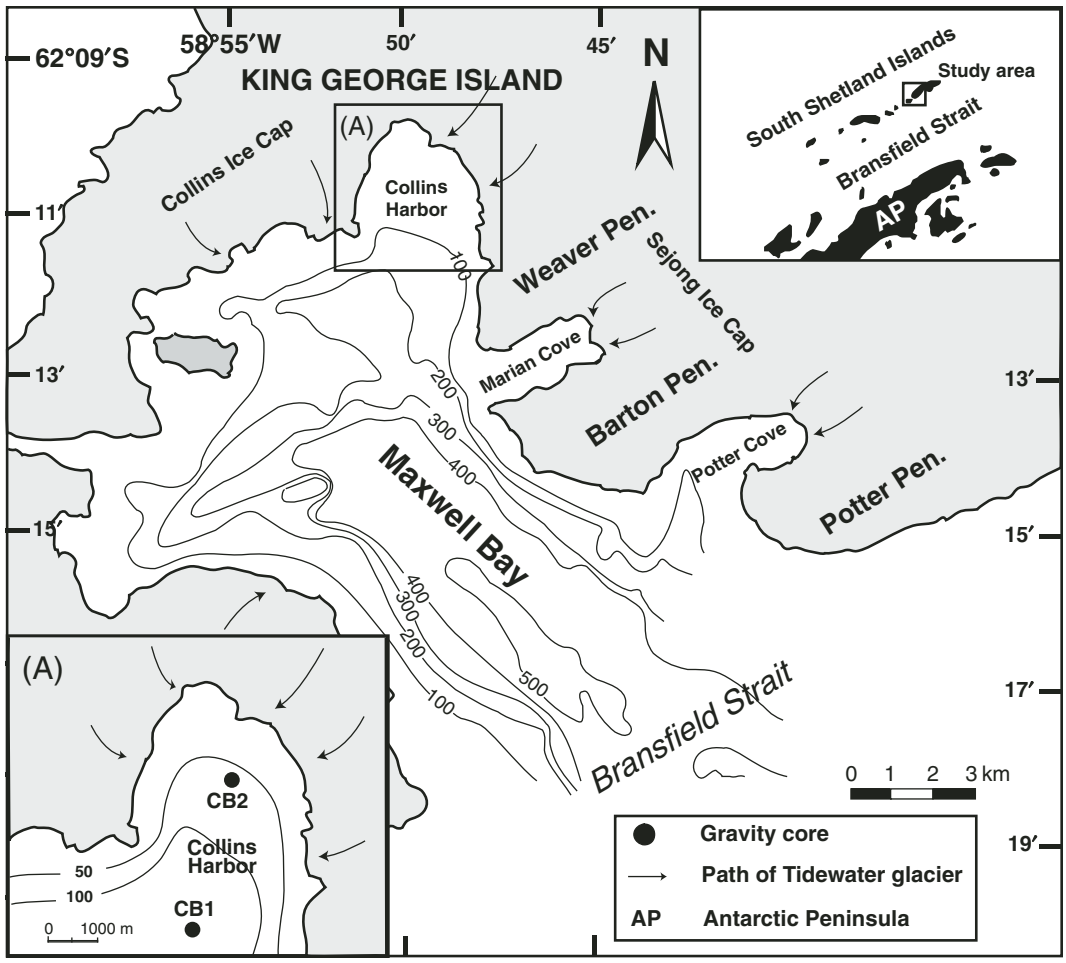

Figure 1. Location map of Maxwell Bay, showing Collins Harbor, Marian and Potter coves, and Collins Ice Cap at the fjord head. Core locations and bathymetry of Collins Harbor in meters are shown in A.

winter, the water column is characterized by a minimum temperature of –1.52 °C and a maximum density of 27.49 kg m^{-3}, indicating that the bay is completely dominated by Weddell Sea Transitional Water (Yoo et al., 2002). The colder Weddell Sea Transitional Water and relatively warmer ACC support different microbiological faunas. The changing dominance of different water masses can be traced over time through the distinctive diatom distributions associated with each water mass.

Glacial History

The Holocene glacial and paleoclimate history of the South Shetland Islands has been reconstructed using various data sets. On the basis of terrestrial evidence, John (1972) and Sugden and Clapperton (1986) suggested that deglaciation in this area began around 10,000 ^{14}C yr B.P. Clapperton and Sugden (1980) also suggested that the South Shetland Islands glaciers are as extensive today as they were 9500 ^{14}C yr B.P. Lake sediment dating indicated that King George Island deglaciated between 9000 and 5000 ^{14}C yr B.P. (Mäusbacher et al., 1989). In addition, a recent report found that late Holocene advance of the Collins Ice Cap, King George Island, occurred after ~650 cal. yr B.P. (Hall, 2007). However, interpretation of a multichannel seismic profile from Maxwell Bay indicated that ice retreat from the bay began ~17,000 ^{14}C yr B.P. (Yoon et al., 1997). This timing is nearly equivalent to that of deglaciation on the Antarctic Peninsula as discussed by Thomas (1979) and Payne et al. (1989), but significantly earlier than deglaciation of the inner shelf of the western Antarctic Peninsula at 13,000 ^{14}C yr B.P. (Heroy and Anderson, 2005). According to the ^{14}C dates from marine sediments, the deglaciation of Marian Cove occurred after 1300 ^{14}C yr B.P. (Yoon et al., 1997).

Several data sets provide additional details concerning the mid-Holocene history of the South Shetland Islands. For example, Björck et al. (1991a) concluded that a climatic optimum occurred between 3200 and 2700 ^{14}C yr B.P. in Midge Lake on Byers Peninsula, an estimate in agreement with the moss bank data on Elephant Island (Björck et al., 1991b). The moss bank data also suggest colder conditions at 5500–4300 and 3900–3200 ^{14}C yr B.P., and an additional mild period at 4150–3900 ^{14}C yr B.P. Humid conditions could have caused readvance of the glaciers on King George Island ~3000 ^{14}C yr B.P. (Barsch and Mäusbacher, 1986; Mäusbacher et al., 1989). Schmidt et al. (1990) attributed increased allochthonous input to lakes to climatic change between 4700 and 3200 ^{14}C yr B.P.

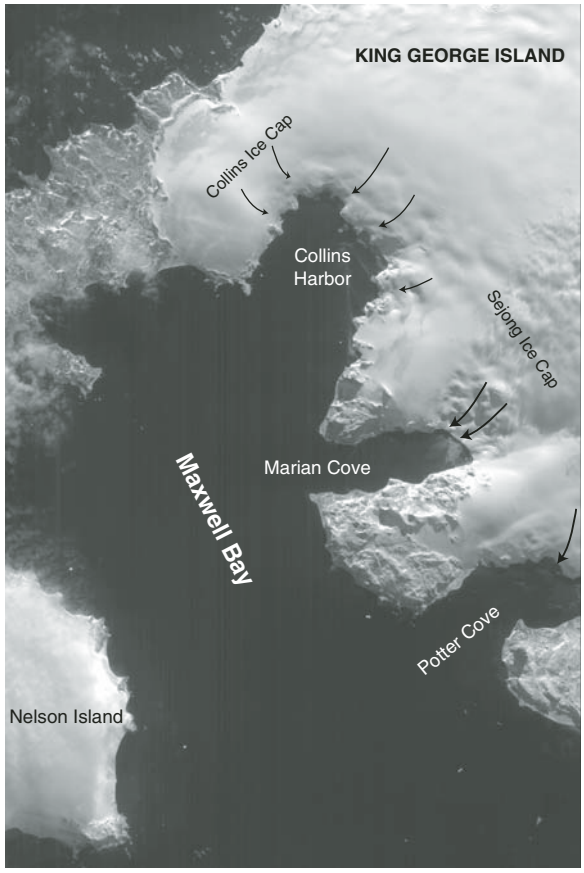

Figure 2. Aerial photo (courtesy of the British Navy) of Maxwell Bay, showing Collins Ice Cap and Marian and Potter coves. Coastal gravel and sand beaches are extensively exposed during the austral summer.

METHODS

Sediment Sampling

Two sediment cores, CB1 and CB2, were collected from the flat seafloor of Collins Harbor, an ice-proximal zone of Maxwell Bay (Fig. 1). Sedimentological, geochemical, and micropaleontological parameters were analyzed to reconstruct paleoenvironmental changes. The two cores were retrieved using a gravity corer and likely recovered the sediment-water interface as determined by examination of X-radiographs from both cores.

Laboratory Analyses

The cores were cut lengthwise in the laboratory; one half was visually described and sliced for X-radiographs, and the other was used for subsampling. Subsamples were taken every 2 cm down the length of the cores to determine total organic carbon (TOC) and calcium carbonate ($CaCO_3$) content, and every 4 cm to determine grain size and diatom assemblage composition and abundance. Grain size distribution for the –4.0–4.0 φ size fractions was analyzed by dry sieving. Finer fractions (σ = 4.0–10.0 φ) were analyzed by a Micrometrics Sedigraph 5000D. The method for computer processing of the raw data has been described by Jones et al. (1988), and the classification of sediments followed Folk and Ward's (1957) scheme. Physical sedimentary and biogenic structures were revealed through X-radiographs of 1-cm-thick sediment slabs. The total carbon (TC) content was measured by a Thermo Finnigan FLASH EA1112 CHNS-O automatic element analyzer. The precision of TC analysis was 3%. The total inorganic carbon (TIC) content was determined by a UIC model 5030 CO_2 coulometer to within 2% precision. The TOC content was calculated as the difference between TC and TIC. Intact micro-shells from core CB1 were used for accelerator mass spectrometry (AMS) radiocarbon dates. The dating was performed by the Nuclear and Geoscience Laboratory of New Zealand. Quantitative diatom analyses for core CB2 were performed by a settling method (Scherer, 1994). This method can be used to determine the absolute diatom concentration (diatoms per gram of sediment). On each slide, ~500 diatom valves were counted along transects, using a Zeiss photomicroscope at a magnification of 1250×. Diatom counts were completed according to the procedures outlined by Schrader and Gersonde (1978).

CHRONOLOGY

Four AMS radiocarbon ages were determined at the Nuclear and Geoscience Laboratory of New Zealand. Radiocarbon dates were obtained from intact calcite shells from four depths of different lithofacies in core CB1 (Table 1). The ages range from 1719 ± 55 ^{14}C yr B.P. at 116 cm depth to 2816 ± 60 ^{14}C yr B.P. at 456 cm depth. No age inversions were observed, implying a lack of reworking during deposition. Although obtained from different lithofacies, the ^{14}C data show a good linear relationship, yielding an average sedimentation rate of 308.1 cm/k.y. (Fig. 3). This implies that there was no significant change in the rate of sediment accumulation during the deposition of core CB1.

Domack and Ishman (1993) reported a similar sedimentation rate of 310 cm/k.y. in Andvord Bay, southwestern Antarctic Peninsula. Assuming a constant rate of sedimentation and confirming recovery of the sedimentary and water interface as corrected by X-radiographs, core CB2 extends back in time ~2000 yr, and upward extrapolation of the linear sedimentation rate results in an assumed age of sediment at the top of the core of ~1370 yr (Fig. 3). Reservoir corrections of ~1300 yr in this study were based on an Antarctic marine reservoir effect of 1300 yr (Berkman et al., 1998). Subtracting the reservoir year of 1300 from the extrapolated core-top age gives an age of ~0 yr for the surface sediments. It is important to keep in mind that these data give only approximate ages for events occurring downcore, because variability in sedimentation rate is possible.

TABLE 1. RESULTS OF ACCELERATED MASS SPECTROMETRY (AMS) ^{14}C DATINGS OF CORE CB1

Core depth (cm)	Age (^{14}C yr B.P.)			Material	Laboratory code
	Uncorrected	Corrected*	Calibrated†		
116	1719 ± 55	419 ± 55	639 ± 55	Micro-shell	NZA15244
210	2001 ± 60	701 ± 60	901 ± 60	Micro-shell	NZA15245
355	2485 ± 60	1185 ± 60	1362 ± 60	Micro-shell	NZA15246
456	2816 ± 65	1516 ± 65	1747 ± 65	Micro-shell	NZA15247

*A 1300-yr correction was applied to all ages of core CB1. This correction appears to be justified because all of the radiocarbon ages in core CB1 increase progressively downcore. This correction is also based upon the fact that the Antarctic marine reservoir effect averages 1300 yr (Berkman et al., 1998).

†All uncorrected ^{14}C dates have been calibrated to calendar years at the two-sigma confidence level using the CALIB program (version 5.0.1) (Stuiver et al., 2005) updated with the marine04.14c dataset (Hughen et al., 2004).

SEDIMENTOLOGY AND GEOCHEMISTRY

Cores CB1 and CB2 were collected from ~3 and ~2 km from the modern calving line of the Collins Ice Cap Glacier in water depths of 120 and 75 m, respectively (Fig. 1A). High-resolution (3.5 kHz) seismic profiles from Collins Harbor at the innermost part of Maxwell Bay show that the seafloor is highly rugged and covered by a thin (<6 m) sediment drape (Yoon et al., 1997). Detailed sedimentological analyses and X-radiography demonstrate that the sedimentary facies alternate between stratified diamicton facies (sD) and massive diamicton facies (mD). Diamicton in this paper refers to a poorly sorted admixture of clast, sand, and mud without a genetic connotation (Eyles et al., 1983; Moncrieff and Hambrey, 1990). Diamictons are all matrix supported but are classified as clast poor, if they have a volume percent of clasts (>2 mm) between 1% and 5%. Clast-rich diamictons are 5%–85% clasts. The matrix is generally fine-grained, with 3%–40% sand and up to 57% mud. Contacts with the facies, both above and below diamicton units, are gradational (Fig. 4).

Stratified Diamicton (sD)

The stratified diamicton facies is made up of alternating clast-poor diamicton layers (Dp) and weakly laminated mud layers (Fl) with occasional homogeneous mud (Fm) (Fig. 4A). This facies is itself weakly laminated, and there is also limited evidence of lamination within some mud layers. The mud layers are usually 1–5 cm thick. Clast-poor diamicton layers (Dp) range from 4 to 6 cm thick (Fig. 4A). The stratified diamicton facies, representing the alternation of Dp and Fl/Fm, is between 90 and 100 cm thick (Figs. 5 and 6). The repeated alternation between Dp and Fm produces the visually laminated appearance of the facies (Fig. 4A). Stratification within the mud layers is formed by millimeter-scale interlamination with black to dark greenish gray (5GY4/1) sand, silt, and silt stringers. Thin silt laminae are more or less parallel to each other but poorly defined and laterally discontinuous and have gradational contacts with the surrounding laminae (Fig. 4A). Current-induced structures are not observed, but load structures occur at the base of some silt horizons (Fig. 4A). Bioturbation is weak to moderate throughout the stratified diamicton facies (less than 10% bioturbated). Clasts are usually concentrated in patches and occasionally show a weak subhorizontal preferred orientation (Fig. 4A). They consist of angular to subangular pebbles to cobbles, ranging from 1 to 7 cm in size, and are mostly composed of andesite, quartz diorite, and andesitic tuff. The matrix, which contains weakly developed laminae, is composed of poorly sorted (σ = 2.5–4.0 φ), sandy to silty clay and shows a heterogeneous texture with a mean grain size of 5.0–9.5 φ (Figs. 5 and 6). The content of TOC is lower than in the surrounding massive diamicton facies (mD) (Figs. 5 and 6). Similarly, the carbon to nitrogen (C/N) ratio is also low compared to mD (Figs. 5 and 6). The absolute abundance of diatom valves is slightly higher in the sD than in the mD (Fig. 7).

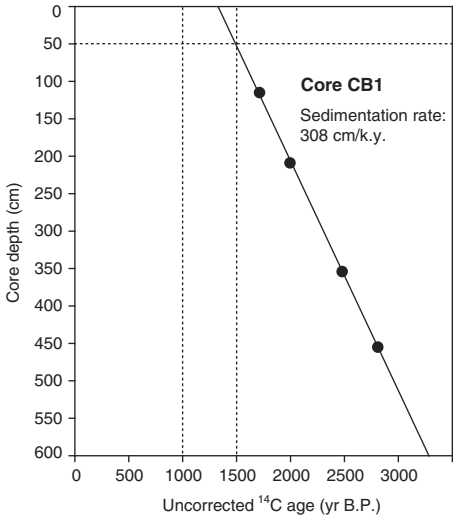

Figure 3. Downcore variations in the uncorrected ^{14}C age and sedimentation rate of core CB1. An average sedimentation rate of 308.1 cm/k.y. is derived from the age versus depth plot.

Massive Diamicton (mD)

The massive diamicton facies (mD) is composed of alternating pale gray (5Y 7/3) clast-rich diamicton layers (Dr) and homogeneous mud layers (Fm) (Fig. 4B). This facies is heterogeneous, poorly sorted, and unstratified, with slightly higher gravel content than the stratified diamicton facies (sD) (Figs. 5 and 6). There is no evidence of lamination within the massive diamicton facies. Rather, bioturbation prevails, as indicated by X-radiographs (Fig. 4B). Clasts of variable sizes are generally scattered but are occasionally concentrated in patches (Fig. 4B). The clasts consist of angular to subangular pebbles to cobbles, ranging from 1 to 7 cm in size. The clasts are randomly oriented and mostly composed of andesite and quartz diorite. Maximal sand content is usually observed in the massive diamicton facies (Figs. 5 and 6). The matrix is homogeneous but partly mottled and predominantly consists of poorly sorted

silty clay, with mean grain sizes of 6.0–8.7 φ in CB1 and 3.1–7.8 φ in CB2 (Figs. 5 and 6). The TOC content in the matrix is exceptionally high (0.16%–0.75% in CB1 and 0.06%–1.12% in CB2) with maximum values at ~455 cm depth in CB2, compared with the surrounding stratified diamicton facies (Figs. 5 and 6). Ratios of C/N are also much higher (5–40 in CB1 and 0–30 in CB2) compared to sD (Figs. 5 and 6). In this facies, sand content tends to be increased (~1%–9% in CB1 and 5%–35% in CB2), and, similarly, gravel content also shows increasing values up to 15% in CB1 and 40% in CB2 (Figs. 5 and 6). Diatom abundance is relatively low compared to its abundance in the stratified diamicton facies (Fig. 7).

MICROPALEONTOLOGY

Diatom abundance in core CB2 varies from 0 to 23 × 10^3 valves per gram dry sediment (Fig. 7). The diatom assemblage is dominated by *Chaetoceros* resting spores (65%–90% of the total). The rest of the assemblages include taxa such as *Fragilariopsis curta* and *Fragilariopsis cylindrus* (Fig. 7). These species have been grouped as sea-ice taxa due to their association with sea-ice and/or sea-ice–related environments (Gersonde, 1986; Zielinski and Gersonde, 1997; Kang et al., 1999). Another interesting component of the diatom assemblage is *Corethron criophilum* (Fig. 7). This species generally occurs in open waters, with less ice cover, such as found in the northern Bransfield Strait, although *Corethron* has been reported from late season sub-ice in the Weddell Sea (Fryxell et al., 1987). Thus their enrichment in the sediment may be related to an episode of early season warmth, resulting in open-water primary production under conditions of strong water column stratification.

Diatom abundance data are shown in Figure 7. Since the large numbers of *Chaetoceros* resting spores in the sediment may mask the signal of the rest of the assemblage, we calculated the relative abundance of the rest of the diatoms excluding the *Chaetoceros* resting spores. The number of diatom valves per unit of sediment (grams) differs somewhat within the facies; the maximum abundance is higher, ranging from 0 to 23 × 10^3 diatoms per gram, in the stratified diamicton facies (sD). In contrast, the number of diatom valves per unit is slightly lower, ranging from 0 to 21 × 10^3 diatoms per gram, in the massive diamicton facies (mD) (Fig. 7). The relative abundance of *Fragilariopsis curta*, a sea-ice diatom, is somewhat high in mD, reaching a distinctive maximum at 120–130 cm (Fig. 7). The abundance of *F. cylindrus* generally follows the same pattern as that of *F. curta*, with a slightly higher abundance in mD than in sD (Fig. 7). *Corethron criophilum* is less abundant than *F. curta* and *F. cylindrus* and is generally more abundant in sD (Fig. 7).

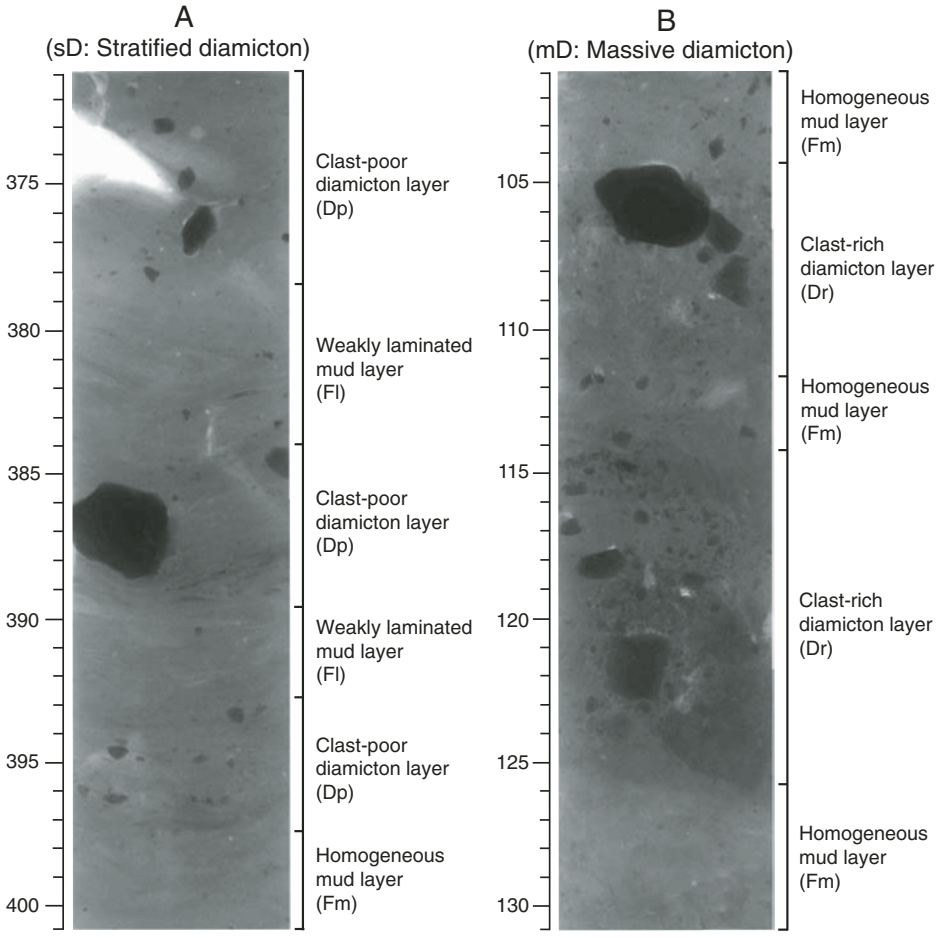

Figure 4. Representative lithofacies observed in core CB1 from Collins Harbor in Maxwell Bay. All scales refer to depth in the core. (A) X-radiograph from core CB1 showing stratified diamicton facies (sD), which alternate between clast-poor diamicton layers (Dp) and weakly laminated mud layers (Fl) with occasional homogeneous mud layers (Fm). (B) X-radiograph from core CB1, showing massive diamicton facies (mD), which alternate between clast-rich diamicton layers (Dr) and homogeneous mud layers (Fm).

INTERPRETATION AND DISCUSSION

Cores from Collins Harbor, an ice-proximal zone of Maxwell Bay, exhibit repeated couplets of organic-rich massive diamicton facies (mD) and organic-poor stratified diamicton facies (sD) (Figs. 5 and 6). The massive diamicton facies is subdivided into clast-rich diamicton layers (Dr) and bioturbated homogeneous mud layers (Fm) (Fig. 4B). The clast-rich diamicton layer is the most difficult sediment to interpret, primarily because it has inherited characteristics of both marine and glacial processes. It is massive and commonly clast-enriched with an unsorted mixture of clay, silt, and gravel, and shows a gradational contact with the nearby stratified diamicton facies (sD) and/or homogeneous mud layers (Fm). These characteristics suggest that the clast-rich diamicton layers originated either as a subglacial till (Anderson et al., 1991) or as ice-proximal glaciomarine deposits in the grounding glaciers. However, a glaciomarine interpretation is supported by the presence of diatoms and the variability in their abundance in the clast-rich diamicton layer (Dr), and by textural heterogeneity (Figs. 5–7), which is an indicator of glaciomarine diamictons (Shevenell et al., 1996; Licht et al., 1999). The variable nature of this facies results from variations in marine productivity and the rate of sediment delivery by iceberg rafting. In particular, the variations in pebble and/or gravel abundance within the massive diamicton layer (Figs. 4–6) provide

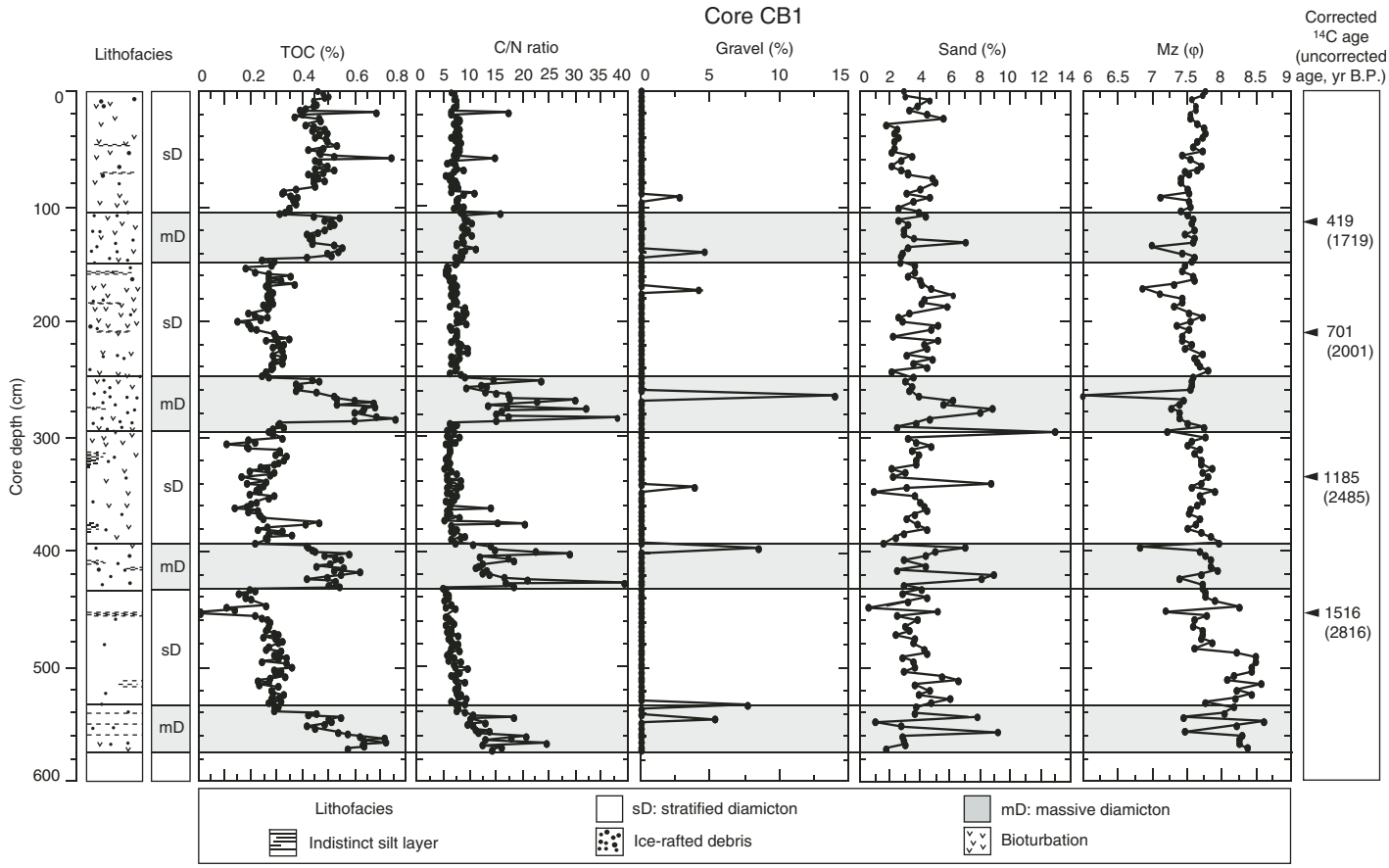

Figure 5. Downcore variations of core CB1 showing the lithofacies, total organic carbon, carbon to nitrogen (C/N) ratio, percentages of gravel and sand, and mean grain size of the matrix in sediments. Corrected ^{14}C ages in yr B.P. are also shown. TOC—total organic carbon.

evidence that the clast-rich diamicton layer (Dr) was deposited in a glaciomarine environment because the flux of ice-rafted material to the seafloor almost certainly varies with time. In contrast, sediment deposited subglacially may be homogenized due to mechanical mixing (e.g., Anderson et al., 1984). Graded sediment and/or interbedding with sandy lenses (turbidites) were not observed, indicating that these glaciomarine diamictons were not reworked by sediment gravity flows (Eyles, 1990). Modern examples of clast-rich massive diamictons formed by iceberg rafting have been reported from East Greenland (Dowdeswell et al., 1994). In that subpolar setting, the concentration of coarse sediment (>2 mm) greatly exceeds that of the fine fraction because of the lack of glaciofluvial discharge, thus producing a poorly sorted admixture of clasts, sand, and mud. Therefore, the clast-rich massive diamicton (Dr) in the present study is interpreted as a product of iceberg delivery of sediments in Maxwell Bay when the rate of fine-grained sediment delivery from turbid meltwater was suppressed but the flux of icebergs across the core sites continued in the fjord system. Bioturbated homogeneous mud layers (Fm) with a few dropstones, which alternate with the clast-rich diamicton layers (Dr) to produce a massive diamicton facies (mD), are interpreted to represent intervals of increased sea-ice cover with suppressed sediment-laden meltwater flux. In contrast, the clast-rich diamicton layer (Dr) probably represents intervening times of more open conditions and iceberg rafting.

Given that numerous icebergs appear to have produced massive diamicton facies, the presence of stratified diamicton facies (sD), which are comprised of clast-poor diamicton layers (Dp) and weakly laminated mud layers (Fl), implies a change in the nature and rate of the operating processes. It is proposed that the stratified diamicton facies (sD) is produced when meltwater discharge is at a maximum with moderate iceberg rafting. During times of climatic warming, when the glacier front has calved significantly and the ice front has retreated, large quantities of glaciofluvial sediment are discharged into the fjord near tidewater termini, resulting in the stratified diamicton facies as found in, for example, Alaska and the South Shetland Islands in Antarctica (Cowan et al., 1997; Yoon et al., 1997). A substantial increase in the rate of fine-grained sediment delivery from glacial meltwater occurred in times of climatic warming and, therefore, effectively swamped the contribution from iceberg sedimentation to produce stratification in the stratified diamicton facies, as happens today in some fjords of the Norwegian island of Spitsbergen during summer (Cowan et al., 1997). This scenario is unlike the fjords of Greenland where the laminated sedimentary units were deposited in times of climatic cooling (i.e., the Younger Dryas and Little Ice Age) when the flux of icebergs was suppressed, but turbid meltwater discharge continued to produce laminations (Dowdeswell et al., 2000).

This stratified diamicton facies is present in both cores, but the stratification appears to be more distinct in core CB2 collected close to the glacier front (Figs. 1 and 4A). There are several possibilities for the origin of the stratification, including current sorting of iceberg-rafted sand and mud during deposition (Orheim and Elverhøi, 1981; Gilbert, 1990) and reworking and winnowing of fine-grained sediments by

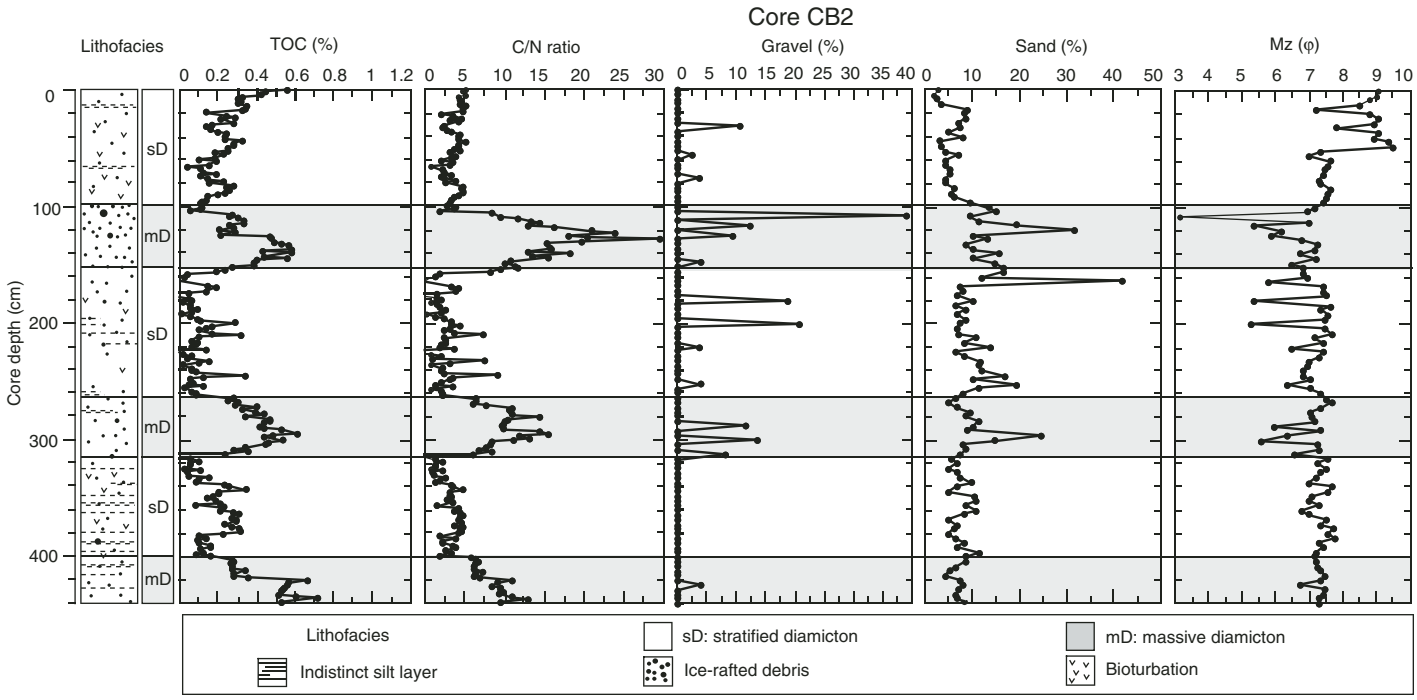

Figure 6. Downcore variations of core CB2 showing the lithofacies, total organic carbon, carbon to nitrogen (C/N) ratio, percentages of gravel and sand, and mean grain size of the matrix in sediments. TOC—total organic carbon.

traction currents after deposition (Eyles et al., 1985). However, in the absence of ripples formed by traction currents, we prefer the former interpretation. We propose that stratification resulted as the volume of subglacial meltwater discharge significantly increased in the ice-proximal zones of Maxwell Bay during phases of climatic warming. Evidence that stratified diamictons (sD) were deposited in times of climatic warming is found in the diatom assemblages of core CB2. The absolute abundance of diatom valves is consistently higher in the stratified diamicton facies (sD) than in the massive diamicton facies (mD) (Fig. 7). This higher abundance of diatom valves is consistent with the observation of the higher number of *Chaetoceros* resting spores in the stratified diamicton facies (Fig. 7). The diatom data indicate that relatively high primary productivity under open marine conditions characterized the environment that gave rise to the deposition of the diatom-rich stratified diamicton facies. Periods of reduced sea-ice cover may have allowed for the incursion of the open-water species *Corethron criophilum* into Maxwell Bay during the deposition of the stratified diamictons (Fig. 7). Subglacial meltwater may also have helped stratify the water column, which may have been favorable for *Corethron* spp. This interpretation is corroborated by the reduced abundance of sea-ice species, *F. curta* and *F. cylindrus*, in the stratified diamictons (Fig. 7).

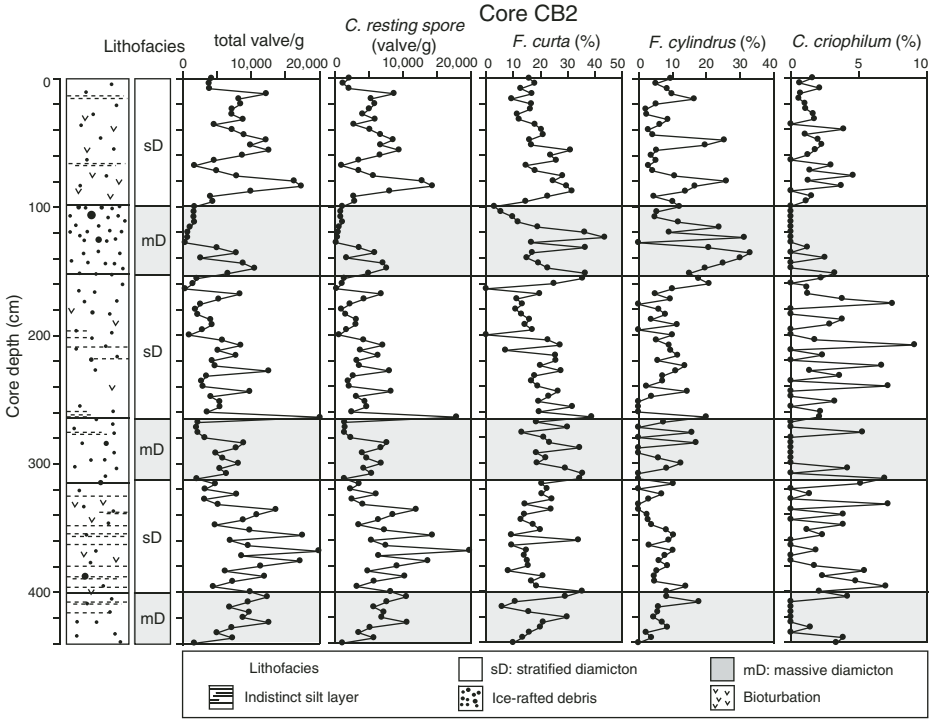

Figure 7. Downcore floral data for core CB2. Absolute diatom concentration, in numbers of valves per gram of sediment and *Chaetoceros* resting spores, and relative abundances of *Fragilariopsis curta*, *Fragilariopsis cylindrus*, and *Corethron criophilum* are plotted versus depth in centimeters.

The organic carbon trend in core CB2 differs from the diatom trend. The massive diamicton facies (mD) has a consistently high TOC content and C/N ratio and a lower absolute abundance of diatom valves (Figs. 6 and 7), whereas the stratified diamicton facies (sD) has a lower TOC content and C/N ratio and higher diatom abundance (Figs. 6 and 7). We suggest that as the climatic conditions deteriorated, turbid meltwater discharge was reduced due to a reduction in the volume of glacial meltwater. Consequently, iceberg rafting became the dominant process for sediment delivery, resulting in the deposition of massive diamicton facies. Gravel and sand were released from icebergs as they melted or rolled, as indicated from the distinct maxima in gravel and sand content in massive diamicton facies (mD) (Figs. 5 and 6). During this period, the core sites experienced relatively high sea-ice cover, which suppressed biological productivity in the water column, as indicated by the reduction of the lower diatom abundance and the reduced contribution of *Chaetoceros* resting spores (Fig. 7). Iceberg rafting and scouring by sea ice, particularly shorefast sea ice during the melting season, were likely major modes of particle transportation in Maxwell Bay during cold climatic periods. These potential processes are also important for the dispersal of coastal benthic macroalgae and/or benthic plants. A modern example of the contribution of sea-ice sediments to the deeper basin has been reported from the Latev Sea in the Arctic (Nürnberg et al., 1994; Darby, 2003), where benthic shallow-water organisms were incorporated into sea-ice cover via frazil and anchor-ice formation. Currently, macroalgal flora with high C/N ratios grow on the coasts of Maxwell Bay; the C/N ratios range from 4 to 16, higher than those of phytoplankton (Weykam and Wiencke, 1996), indicating that coastal algae is probably a main source for the organic carbon with an elevated C/N ratio in the massive diamicton facies (Figs. 5 and 6). However, the C/N ratio of the massive diamicton units ranges from 15 to 30, up to twice the C/N ratios of modern benthic algae in Maxwell Bay (Weykam and Wiencke, 1996). This high C/N ratio may reflect limited N availability during the deposition of the massive diamicton facies (mD). In general, C/N ratios are regarded as being dependent on nutrient availability (Atkinson and Smith, 1983; Levitt and Bolton, 1990; Neori et al., 1991; Delgado et al., 1994). For example, red algae from the South African west coast, a nutrient-rich upwelling system, showed similarly low C/N ratios, between 7 and 12 (Levitt and Bolton, 1990), to the modern Antarctic species. Thus the decreased N content and elevated C/N ratios measured in the massive diamicton facies (mD) (Figs. 5 and 6) may be interpreted as a result of reduced N availability in Maxwell Bay bottom water in times of cold climate when formation of extensive sea ice suppressed the upwelling of Antarctic water, which has high and constant N content throughout the year. McMinn (2000) examined marine sediment cores from the Abel fjords, eastern Antarctica, and suggested that the elevated C/N ratio in cores resulted from a more restricted and isolated N-limiting environment during the increase in sea-ice cover. However, the inability to track the signature of the macroalgal debris in the sediment cores precludes more precise interpretation for the greater input of macroalgal debris during intervals of cooling.

WIDER PALEOCLIMATIC IMPLICATIONS

The cores collected from the ice-proximal zone in Maxwell Bay are marked by distinct cyclical fluctuations in TOC content with generally higher C/N ratios and lower numbers of diatom valves in the massive diamicton facies (mD) (Figs. 5–7). We propose that this high flux of organic carbon is related to the delivery of macroalgal plants growing in the coastal zone via sea-ice entrainment in times of climatic cooling. The high flux of organic carbon during the deposition of the massive diamicton could reflect periods of decreased terrigenous sedimentation. However, peaks in the sand content in the massive diamictons from the cores reflect the advance of the calving glacier and consequent increased terrigenous input (Figs. 5 and 6). Thus the TOC maxima would indicate climatic cold periods, and the minima indicate warmer periods. Distinct maxima and minima in TOC content repeat about every 130 cm in core CB1 and every 100 cm in core CB2 (Figs. 5 and 6). The chronology of core CB2 is constrained by AMS ^{14}C data, which demonstrate an average sedimentation rate of ~310 cm/kyr. The cyclical pattern in the TOC content in core CB2 has an approximate 500 yr periodicity. Therefore, the peaks of TOC content, as interpreted by the C/N ratio and diatom assemblage data, suggest that the glacier front in Collins Harbor, an ice-proximal zone of Maxwell Bay, advanced periodically at a time interval of ~500 yr due to either climatic cooling or the absence of warm Circumpolar Deep Water (CDW). In comparison with nearby terrestrial data reported by Hall (2007), these records may shed light on consistency in the proposed environmental changes. Currently, however, we have no explanation for the forcing mechanism responsible for the pronounced cyclicity, because comparative paleoclimatic cooling records with 500 yr cyclicity are rare for the Southern Hemisphere (Warner and Domack, 2002; Costa et al., 2007). Modern Maxwell Bay is filled with warm CDW, which has a temperature of greater than 1 °C (Chang et al., 1990). This relatively warm CDW may provide a heat source to surface waters, especially during periods of greater CDW upwelling, resulting in decreased sea-ice extent (Jacobs and Comiso, 1993) and ice-front melting. In the absence of CDW, ice-front melting would be expected to be significantly less than it is at present. A sediment core study from the Müller Ice Shelf on the southwestern Antarctic Peninsula suggested that glacier-front advance may be linked to the exclusion of CDW from the fjord (Domack et al., 1995). It is, therefore, suggested that the absence of CDW contributed to the advance of glacier margins in Maxwell Bay during the late Holocene. A decrease in CDW in the Southern Ocean may be correlative with the high-frequency (550 yr) variability in reduced North Atlantic Deep Water (NADW) production during cold climatic conditions (Chapman and Shackleton, 2000). The reasoning behind this speculation is mainly that a change in the intensity or distribution of NADW, mixed efficiently with water masses of the Antarctic Circumpolar Current (ACC) system to form CDW, may reflect the changing influence of CDW through time. The production of NADW was found to be decreased during the glacial periods throughout the Pleistocene (Broecker and Denton, 1989; Charles and Fairbanks, 1992). The age model is consistent with the natural, 500 yr cooling cycle documented during the late Holocene (Chapman and Shackleton, 2000). However, the lack of a strong cooling signal with elevated C/N ratios and TOC content at the core top is surprising, since, in order of timing, the top of core CB1 may document a return to cold climate. Potentially, the recent unprecedented warming in the Antarctic Peninsula may be responsible for dampening the effect of the natural climatic cooling (Domack et al., 2005). However, the imprecision of dating techniques precludes more precise interpretation of this apparent lack of a strong cooling signal.

ACKNOWLEDGMENTS

We would like to thank C.Y. Kang, I.K. Um, and S.Y. Im for their sincere efforts during the 2002–2003 Korea Antarctic Research Program (KARP) cruise to the South Shetland Islands. We also are grateful to the crew of R/V *Yuzhmorgeologya* for all their help during the gravity coring on board. This research was mostly funded as Korea Polar Research Institute (KOPRI) grant PE09010.

REFERENCES CITED

Anderson, J.B., Brakes, C.F., and Mayers, N.C., 1984, Sedimentation on the Ross Sea continental shelf, Antarctica: Marine Geology, v. 57, p. 295–333, doi: 10.1016/0025-3227(84)90203-2.

Anderson, J.B., Kennedy, D.S., Smith, M.J., and Domack, E.W., 1991, Sedimentary facies associated with Antarctica's floating ice masses, *in* Anderson, J.B., and Ashley, G.M., eds., Glacial Marine Sedimentation, Paleoclimatic Significance: Boulder, Colorado, Geological Society of America Special Paper 261, p. 1–25.

Atkinson, M.J., and Smith, S.V., 1983, C:N:P ratios of benthic marine plants: Limnology and Oceanography, v. 28, p. 568–574.

Barsch, D., and Mäusbacher, R., 1986, New data on the relief development of the South Shetland Islands, Antarctica: Interdisciplinary Science Reviews, v. 11, p. 211–218.

Berkman, P.A., Andrew, J.T., Björck, S., Colhoun, E.A., Emslis, S., Goodwin, I.D., Hall, B.L., Hart, C.P., Hirakawa, K., Igarashi, A., Ingólfson, O., López-Martínez, J., Lyons, W.B., Mabin, M.C.G., Quilty, P.G., Taviani, M., and Yoshida, Y., 1998, Circum-Antarctic coastal environmental shifts during the Late Quaternary reflected by emerged marine deposits: Antarctic Science, v. 10, p. 345–362, doi: 10.1017/S0954102098000406.

Björck, S., Håkansson, H., Zale, R., Karlén, W., and Liedberg Jönsson, B., 1991a, A late Holocene lake sediment sequence from Livingston Island, South Shetland Islands, with paleoclimatic implications: Antarctic Science, v. 3, p. 61–72, doi: 10.1017/S095410209100010X.

Björck, S., Malmer, N., Hjort, C., Sandgren, P., Ingólfsson, O., Wallén, B., Lewis Smith, R.I., and Liedberg Jönsson, B., 1991b, Stratigraphic and paleoclimatic studies of a 5500-year-old moss bank on Elephant Island, Antarctica: Arctic and Alpine Research, v. 23, p. 361–374, doi: 10.2307/1551679.

Broecker, W.S., and Denton, G.H., 1989, The role of ocean-atmosphere reorganization in glacial cycles: Geochimica et Cosmochimica Acta, v. 53, p. 2465–2501, doi: 10.1016/0016-7037(89)90123-3.

Chang, K.I., Jun, H.K., Park, G.T., and Eo, Y.S., 1990, Oceanographic condition of Maxwell Bay, King George Island, Antarctica (austral summer, 1989): Korea Journal of Polar Research, v. 1, p. 27–46.

Chapman, M.R., and Shackleton, N.J., 2000, Evidence of 550-year and 1000-year cyclicities in North Atlantic circulation patterns during the Holocene: The Holocene, v. 10, p. 287–291, doi: 10.1191/095968300671253196.

Charles, C.D., and Fairbanks, R.G., 1992, Evidence from Southern Ocean sediments for the effect of North Atlantic deep-water flux on climate: Nature, v. 355, p. 416–419, doi: 10.1038/355416a0.

Clapperton, C.M., and Sugden, D.E., 1980, Geomorphology of the St. Andrews Bay–Royal Bay area, South Georgia: British Antarctic Survey Miscellaneous Map Series Sheet 1.

Costa, E., Dunbar, R.B., Kryc, K.A., Mucciarone, D.A., Brachfeld, S., Roark, E.B., Manley, P.L., Murray, R.W., and Leventer, A., 2007, Solar forcing and El Niño–Southern Oscillation (ENSO) influences on productivity cycles interpreted from a late Holocene high-resolution marine sediment record, Adélie Drift, East Antarctic Margin, *in* Cooper, A., Raymond, C., and the International Symposium on Antarctic Earth Sciences Editorial Team, eds., Antarctica: A Keystone in a Changing World—Online Proceedings for the Tenth International Symposium on Antarctic Earth Sciences: U.S. Geological Survey Open-File Report 2007-1047, 36 p., doi: 10.3133/of2007-1047.srp036.

Cowan, E.A., Cai, J., Powell, R.D., Clark, J.D., and Pitcher, J.N., 1997, Temperate glaciomarine valves: An example from Disenchantment Bay, Southern Alaska: Journal of Sedimentary Research, v. 67, p. 536–549.

Darby, D.A., 2003, Sources of sediment found in sea ice from the western Arctic Ocean, new insights into processes of entrainment and drift patterns: Journal of Geophysical Research, v. 108, p. 3257, doi: 10.1029/2002JC001350.

Delgado, O., Ballesteros, E., and Vidal, M., 1994, Seasonal variation in tissue nitrogen and phosphorus of *Cystoseira mediterranea* Sauvageau (Fucales, Phaeophyceae) in the Northwestern Mediterranean Sea: Botanica Marina, v. 37, p. 1–9.

Domack, E.W., and Ishman, S.E., 1993, Oceanographic and physiographic controls on modern sedimentation within Antarctic fjords: Geological Society of America Bulletin, v. 105, p. 1175–1189, doi: 10.1130/0016-7606(1993)105<1175:OAPCOM>2.3.CO;2.

Domack, E.W., Ishman, S.E., Stein, A.B., McClennen, C.E., and Timothy Jull, A.J., 1995, Late Holocene advance of the Müller Ice Shelf, Antarctic Peninsula: Sedimentological, geochemical and paleontological evidence: Antarctic Science, v. 7, p. 159–170, doi: 10.1017/S0954102095000228.

Domack, E.W., Duran, D., Leventer, A., Ishman, S., Doane, S., McCallum, S., Amblas, D., Ring, J., Gilbert, R., and Prentice, M., 2005, Stability of the Larsen B ice shelf on the Antarctic Peninsula during the Holocene epoch: Nature, v. 436, p. 681–685, doi: 10.1038/nature03908.

Dowdeswell, J.A., Whittington, R.J., and Marienfeld, P., 1994, The origin of massive diamicton facies by iceberg rafting and scouring, Scoresby Sund, East Greenland: Sedimentology, v. 41, p. 21–35, doi: 10.1111/j.1365-3091.1994.tb01390.x.

Dowdeswell, J.A., Whittington, R.J., Jennings, A.E., Andrews, J.T., Mackensen, A., and Marienfeld, P., 2000, An origin for laminated glaciomarine sediments through sea-ice build-up and suppressed iceberg rafting: Sedimentology, v. 47, p. 557–576, doi: 10.1046/j.1365-3091.2000.00306.x.

Eyles, N., 1990, Marine debris flows: Late Precambrian "tillites" of the Avalonian-Cadomian orogenic belt: Palaeogeography, Palaeoclimatology, Palaeoecology, v. 79, p. 73–98, doi: 10.1016/0031-0182(90)90106-H.

Eyles, N., Eyles, C.H., and Miall, A.D., 1983, Facies types and vertical profile model: An alternative approach to the description and environmental interpretation of glacial diamict and diamictic sequences: Sedimentology, v. 30, p. 393–410, doi: 10.1111/j.1365-3091.1983.tb00679.x.

Eyles, C.H., Eyles, N., and Miall, A.D., 1985, Models of glaciomarine sedimentation and their application to the interpretation of ancient glacial sequences: Palaeogeography, Palaeoclimatology, Palaeoecology, v. 51, p. 15–84, doi: 10.1016/0031-0182(85)90080-X.

Folk, R.L., and Ward, W.C., 1957, Brazos river bars: A study in the significance of grain size parameters: Journal of Sedimentary Petrology, v. 27, p. 3–26.

Fryxell, G.A., Kang, S., and Reap, M., 1987, AMERIEZ 1986: Phytoplankton at the Weddell Sea ice-edge: Antarctic Journal of the United States, v. 22, p. 173–175.

Gersonde, R., 1986, Siliceous microorganisms in sea ice and their record in sediments in the southern Weddell Sea (Antarctica): Proceedings of the Eighth Symposium on Living and Fossil Diatoms, p. 549–566.

Gilbert, R., 1990, Rafting in glaciomarine environments, *in* Dowdeswell, J.A., and Scourse, J.D., eds., Glaciomarine Environments: Processes and Sediments: The Geological Society of London, Special Publication 53, p. 105–120.

Hall, B.L., 2007, Late-Holocene advance of the Collins Ice Cap, King George Island, South Shetland Islands: The Holocene, v. 17, p. 1253–1258, doi: 10.1177/0959683607085132.

Heroy, D.C., and Anderson, J.B., 2005, Ice-sheet extent of the Antarctic Peninsula region during the Last Glacial Maximum (LGM)—Insights from glacial morphology: Geological Society of America Bulletin, v. 117, p. 1497–1512, doi: 10.1130/B25694.1.

Hofmann, E.E., Klinck, J.M., Lascara, C.M., and Smith, D., 1996, Water mass distribution and circulation west of the Antarctic Peninsula and including Bransfield Strait, *in* Ross, R.M., Hofmann, E.E., and Quetin, L.B., eds., Foundations for ecological research west of the Antarctic Peninsula: Washington, D.C., American Geophysical Union, p. 61–80.

Hughen, K.A., Baillie, M.G.L., Bard, E., Beck, J.W., Bertrand, C.J.H., Blackwell, P.G., Buck, C.E., Burr, G.S., Cutler, K.B., Damon, P.E., Edwards, R.L., Fairbanks, R.G., Friedrich, M., Guilderson, T.P., Kromer, B., McCormac, G., Manning, S., Ramsey, C.B., Reimer, P.J., Reimer, R.W., Remmele, S., Southon, J.R., Stuiver, M., Talamo, S., Taylor, F.W., Van Der Plight, J., and Weyhenmeyer, C.E., 2004, Marine04 marine radiocarbon age calibration, 0-26 Cal Kyr BP: Radiocarbon, v. 46, p. 1059–1086.

Jacobs, S.S., and Comiso, J.C., 1993, A recent sea-ice retreat west of the Antarctic Peninsula: Geophysical Research Letters, v. 20, p. 1171–1174, doi: 10.1029/93GL01200.

John, B.S., 1972, Evidence from the South Shetland Islands towards a glacial history of West Antarctica, *in* Price, R.J., and Sugden, D.E., eds., Polar Geomorphology: Institute of British Geographers Special Publication, v. 4, p. 75–92.

Jones, K.P.N., McCave, I.N., and Patel, P.D., 1988, A computer-interfaced sedigraph for modal size analysis of fine-grained sediment: Sedimentology, v. 35, p. 163–172, doi: 10.1111/j.1365-3091.1988.tb00910.x.

Kang, J.-S., Kang, S.-H., and Lee, J.H., 1999, Cryophilic diatoms *Navicula glaciei* and *N. perminuta* in Antarctic coastal environment: Morphology and Ecology: Algae (Korean Phycological Society), v. 14, p. 169–179.

Kim, J.H., Chung, H., Oh, Y.S., and Lee, I.K., 2001, Macroalgal flora of Maxwell Bay, King George Island, Antarctica: I. Cholrophyta, Chrysophyta and Phaeophyta: Ocean and Polar Research, v. 23, p. 209–221.

KOPRI (Korean Polar Research Institute), 2009, Annual weather report (King Sejong, Korean Antarctic station, 2007): Korea Polar Research Institute Open-File Report BSPE08030, p. 17–92.

Levitt, G.J., and Bolton, J.J., 1990, Seasonal primary production of understory Rhodophyta in an upwelling system: Journal of Phycology, v. 26, p. 214–220, doi: 10.1111/j.0022-3646.1990.00214.x.

Licht, K.J., Dunbar, N.W., Andrews, J.T., and Jenning, A.E., 1999, Distinguishing subglacial till and glacial marine diamictons in the western Ross Sea, Antarctica: Implications for a last glacial maximum grounding line: Geological Society of America Bulletin, v. 111, p. 91–103, doi: 10.1130/0016-7606(1999)111<0091:DSTAGM>2.3.CO;2.

Mäusbacher, R., Müller, J., Munnich, M., and Schmidt, R., 1989, Evolution of postglacial sedimentation in Antarctic lakes (King George Island): Zeitschrift für Geomorphologie, v. 33, p. 219–234.

McMinn, A., 2000, Late Holocene increase in sea ice extent in fjords of the Vestfold Hills, eastern Antarctica: Antarctic Science, v. 12, p. 80–88, doi: 10.1017/S0954102000000110.

Moncrieff, A.C.M., and Hambrey, M.J., 1990, Marginal-marine glacial sedimentation in the late Precambrian succession of East Greenland, *in* Dowdeswell, J.A., and Scourse, J.D., eds., Glacial Environments: Processes and Sediments: The Geological Society of London Special Publication, v. 53, p. 387–410.

Neori, A., Cohen, I., and Gordin, H., 1991, *Ulva lactuca* biofilters for marine fishpond effluents. II: Growth rate, yield and C:N ratio: Botanica Marina, v. 34, p. 483–489, doi: 10.1515/botm.1991.34.6.483.

Nürnberg, D., Wollenburg, I., Dethleff, D., Eicken, H., Kassens, H., Letzig, T., Reimniz, E., and Thiede, J., 1994, Sediments in Arctic sea ice—Implications for entrainment, transport and release: Marine Geology, v. 119, p. 185–214, doi: 10.1016/0025-3227(94)90181-3.

Orheim, O., and Elverhøi, A., 1981, Model for submarine glacial deposition: Annals of Glaciology, v. 2, p. 123–127.

Park, B.-K., Chang, S.-K., Yoon, H.I., and Chung, H.S., 1998, Recent retreat of ice cliffs, King George Island, South Shetland Islands, Antarctic Peninsula: Annals of Glaciology, v. 27, p. 633–635.

Payne, J.A., Sugden, D.E., and Clapperton, C.M., 1989, Modeling the growth and decay of the Antarctic Peninsula ice sheet: Quaternary Research, v. 31, p. 119–134, doi: 10.1016/0033-5894(89)90002-1.

Read, J.F., Pollard, R.T., Morrison, A.I., and Symon, C., 1995, On the southerly extent of the Antarctic Circumpolar Current in the southeast Pacific: Deep-sea Research. Part II, Topical Studies in Oceanography, v. 42, p. 933–954, doi: 10.1016/0967-0645(95)00061-T.

Reynolds, J.M., 1981, Distribution of mean annual air temperatures in the Antarctic Peninsula: British Antarctic Survey Bulletin, v. 54, p. 123–133.

Scherer, R.P., 1994, A new method for the determination of absolute abundance of diatoms and other silt-sized sedimentary particles: Journal of Paleolimnology, v. 12, p. 171–179, doi: 10.1007/BF00678093.

Schmidt, R., Mäusbacher, R., and Müller, J., 1990, Holocene diatom flora and stratigraphy from sediment cores of two Antarctic lakes (King George Island): Journal of Paleolimnology, v. 3, p. 55–74, doi: 10.1007/BF00209300.

Schrader, H.J., and Gersonde, R., 1978, Diatoms and silicoflagellates: Uttecht Micropaleontological Bulletin, v. 17, p. 129–176.

Shevenell, A.E., Domack, E.W., and Kernan, G.M., 1996, Record of Holocene paleoclimate changes along the Antarctic Peninsula: Evidence from glacial marine sediments, Lallemand Fjord, *in* Banks, M.R., and Brown, M.J., eds., Climate succession and glacial history over the past five million years: Royal Society of Tasmania 130, p. 55–64.

Smith, B.M.E., 1972, Airborne radio echo soundings of glaciers in the Antarctic Peninsula: British Antarctic Survey Scientific Report 72.

Stuiver, M., Reimer, P.J., and Reimer, R., 2005, CALIB Radiocarbon Calibration (HTML Version 5.0) http://radiocarbon.pa.qub.ac.uk/calib/.

Sugden, D.E., and Clapperton, C.M., 1986, Glacial history of the Antarctic Peninsula and South Georgia: South African Journal of Science, v. 82, p. 508–509.

Thomas, R.H., 1979, West Antarctic ice sheet: Present-day thinning and Holocene retreat of the margins: Science, v. 205, p. 1257–1258, doi: 10.1126/science.205.4412.1257.

Vaughan, D.G., Marshall, G.J., Connolley, W.M., Parkinson, C., Mulvaney, R., Hodgson, D., King, J., Pudsey, C., and Turner, J., 2003, Recent rapid regional climatic warming on the Antarctic Peninsula: Climatic Change, v. 60, p. 243–274, doi: 10.1023/A:1026021217991.

Warner, N.R., and Domack, E.W., 2002, Millennial- to decadal-scale paleoenvironmental change during the Holocene in the Palmer Deep, Antarctica, as recorded by particle-size analysis: Paleoceanography 17, no. 3, p. 8004, doi: 10.1029/2000PA000602.

Weykam, G., and Wiencke, C., 1996, Seasonal photosynthetic performance of the endemic Antarctic alga *Palmaria decipiens* (Reinsch) Ricker: Polar Biology, v. 16, no. 5, p. 357–361, doi: 10.1007/BF02342184.

Yoo, K.-C., Kang, C.Y., Yoon, H.I., Suk, D.W., and Oh, J.-K., 2002, Seasonal water column properties and dispersal pattern of suspended particulate matter (SPM) in Marian Cove, King George Island: South Shetland Islands: Journal of the Geological Society of Korea, v. 38, p. 573–593.

Yoon, H.I., Han, M.W., Park, B.-K., Oh, J.-K., and Chang, S.-K., 1997, Glaciomarine sedimentation and paleoglacial setting of Maxwell Bay and its tributary embayment, Marian Cove, South Shetland Islands, West Antarctica: Marine Geology, v. 140, p. 265–282, doi: 10.1016/S0025-3227(97)00028-5.

Yoon, H.I., Park, B.-K., Domack, E.W., and Kim, Y., 1998, Distribution and dispersal pattern of suspended particulate matter in Maxwell Bay and its tributary, Marian Cove in the South Shetland Islands, West Antarctica: Marine Geology, v. 152, p. 261–275, doi: 10.1016/S0025-3227(98)00098-X.

Zielinski, U., and Gersonde, R., 1997, Diatom distribution in Southern Ocean surface sediments (Atlantic sector): Implications for paleoenvironmental reconstructions: Palaeogeography, Palaeoclimatology, Palaeoecology, v. 129, p. 213–250, doi: 10.1016/S0031-0182(96)00130-7.

Manuscript Received 26 September 2009
Revised Manuscript Received 15 October 2009
Manuscript Accepted 27 October 2009

Printed in the USA